Dual-polarized Grid-slotted Microstrip Antenna with Enhanced Bandwidth and Low Profile

Wangyu Sun and Yue Li

Department of Electronic Engineering
Tsinghua University, Beijing, 100084, China
sunwy16@mails.tsinghua.edu.cn, lyee@tsinghua.edu.cn

Abstract ─ In this paper, a wideband dual-polarized microstrip antenna is proposed inspired by the concept of the periodic grid-slotted surface. Inherited the merit of low profile from microstrip antenna, a relatively wide bandwidth, i.e., up to 43% with reflection coefficient less than -10 dB, is achieved for both orthogonal polarizations. Multiple modes are excited due to the periodic slot-loaded structure and well matched using crossed aperture-coupled Y-shaped feeding. The overall height of the proposed antenna is only 0.06 λ_0, λ_0 is the free-space wavelength at the centre frequency of 5.5 GHz. The proposed antenna is systematically studied in the numerical simulation and experiment, and results agree well. The proposed dual-polarized antenna provides an effective choice for wideband low profile antenna for the applications of base station.

Index Terms ─ Antenna feeds, microstrip antennas, polarization diversity, wideband antennas.

I. INTRODUCTION

Dual polarized antennas are widely used in modern wireless communication systems, especially for the applications of base stations. Conventional dual polarized antennas applied in base stations are cross-dipoles [1-2] or magneto-electric dipoles [3], which achieve a broad bandwidth around 45%. However, these designs are usually with a high profile above 0.2 λ_0. Therefore, how to decrease the profile (less than 0.1 λ_0) of the dual polarized base station antenna and maintain the broad bandwidth (around 45%) is still a challenge. Microstrip antennas may be a suitable choice to achieve this target due to these obvious advantages of low profile, light weight, low cost and easy integration [4]. Nevertheless, typical microstrip antennas usually suffer from narrow impedance bandwidth, e.g., less than 10% because of the high quality factor [5].

Several methods have been proposed to enhance the bandwidth of microstrip antennas. For example, the bandwidth as high as 20% can be achieved by using thick substrate with low dielectric constant for a low quality factor [6]. Reference [7] presents a microstrip antenna with the impedance bandwidth greater than 20% by embedding a U-shaped slot. E-shaped microstrip antenna fed by a probe is given in [8], demonstrating that the bandwidth could reach up to 30.3%. And the stacked structures have been utilized to provide broadband property, knowing as the stacked microstrip antennas [9]. However, the profiles of these designs are usually higher than 0.1 λ_0. To maintain the low profile performance and improve the bandwidth, multimode coupling theory [10-11] becomes an available method recently. By coupling TM_{10} and TM_{30} modes, the bandwidth of 15.5% is achieved with a profile of 0.03 λ_0 [10]. Nevertheless, not all above techniques are suitable to be applied in dual-polarized applications due to asymmetrical radiating patches or complex feeding networks [11].

In our previous work [12], a microstrip antenna with strip-slotted hybrid patch and aperture-coupling feeding structure is presented. By adding three periodic slots on the radiating aperture, TM_{10} and antiphase TM_{20} modes are excited and coupled to achieve a broadband of 41% with a low profile of 0.06 λ_0. But it can only support one polarization. Inspired from the periodic radiating structure in [12], a dual-polarized microstrip antenna with grid-slotted radiating aperture is proposed to realize the broad bandwidth and low profile. As this design is with a symmetrical radiating aperture, dual polarizations can be excited through the cross coupling-apertures and the cross Y-shaped feeding lines, which also help to realize the wideband characteristic. The antenna sample is fabricated for experiment, exhibiting good agreement with simulation results. The relative bandwidth around 43% for two polarizations and the profile of 0.06 λ_0 indicate the proposed dual-polarized antenna has the potential to be applied in the design of low profile base stations.

II. ANTENNA DESIGN AND ANALYSIS

Figure 1 illustrates the configuration of the proposed dual-polarized grid-slotted microstrip antenna. The grid-

Submitted On: November 2, 2018
Accepted On: December 14, 2018

slotted radiating patch is above the ground and the crossed Y-shaped feeding lines is underneath the ground. Two dielectric layers (ε_r=3.38, μ_r=1 and tan δ=0.0027) with different thicknesses are utilized to support the antenna. The detailed geometry and dimensions are plotted in Figs. 2 (a)-(c) with the optimized parameters listed in Table 1. The proposed antenna is composed of 4×4 small square patch units with identical size and fed through a pair of orthogonal Y-shaped feeding lines. This structure can be regarded as a combination of two orthogonal 1×4 strip-slotted hybrid structures in [12]. Therefore, orthogonal polarizations are excited along *x*- and *y*-axis, respectively. For each Y-shaped feeding line, the distance between the two arms (W) and the vertical distance (s) are tuned for wideband impedance matching. The widths of these sections (W_{ms}, W_{ms2}) are selected to the intrinsic impedance of 50 Ω. To avoid the intersection, four crossover structures with the same dimensions are introduced, and the detailed view is shown in Fig. 2 (c). The vias in the crossover are applied to connect the upper and bottom parts of Microstrip 1 or Microstrip 2. Therefore, the orthogonal Y-shaped feeding lines are separated at the intersecting points.

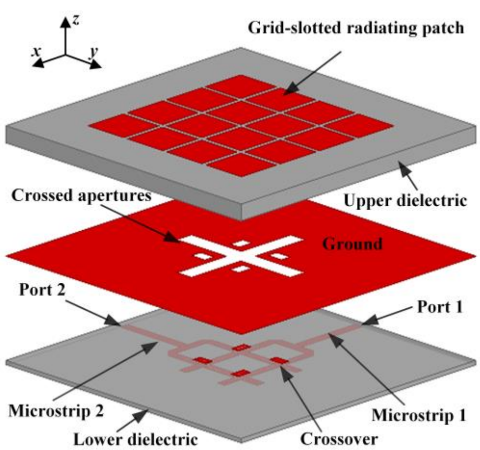

Fig. 1. Perspective view of the proposed dual-polarized grid-slotted microstrip antenna.

The proposed antenna applies the Y-shaped feeding line, instead of the typical straight feeding line. It has two benefits: (1) Improvement on impedance matching; (2) Easy realization of dual polarizations. To validate the design strategy, the evolution processes (Ant. 1, Ant. 2 and Proposed Ant.) are illustrated in Fig. 3, with the comparisons on reflection coefficients. Firstly, extra tuning parameters, i.e., W and s, are provided for impedance matching and lead to a remarkable improvement for impedance bandwidth. For Ant. 1, the simulated impedance bandwidth with |S11|<-10 dB is 4.50-5.92 GHz (27.3%). For Ant. 2, the impedance bandwidth is 4.26-6.54 GHz (42%). The introduction of this Y-shaped microstrip feeding line greatly enhances the relative bandwidth with an increment of 15%. Secondly, the Y-shaped geometry is indispensable to achieve a dual-polarized performance. Supposing two straight microstrip lines are used to create a cross feeding structure, just as shown in Fig. 4 (a), the intersection of two orthogonal straight lines is right underneath the centre of cross apertures. Thus, it is difficult to avoid the intersection, even using the crossover mentioned in Fig. 2 (c). In Fig. 4 (b), two orthogonal Y-shaped microstrip lines are applied and the four intersections move outwards and are away from the cross-coupling apertures. Thus, with the Y-shaped feeding structure and crossovers, the two cross microstrip lines can be separated in the same layer to further excite two orthogonal polarizations. Besides, in Fig. 3, the proposed dual-polarized antenna (Proposed Ant.) can also realize a much wider simulated impedance bandwidth of 4.29-6.40 GHz (39.5%) than Ant. 1 (27.3%).

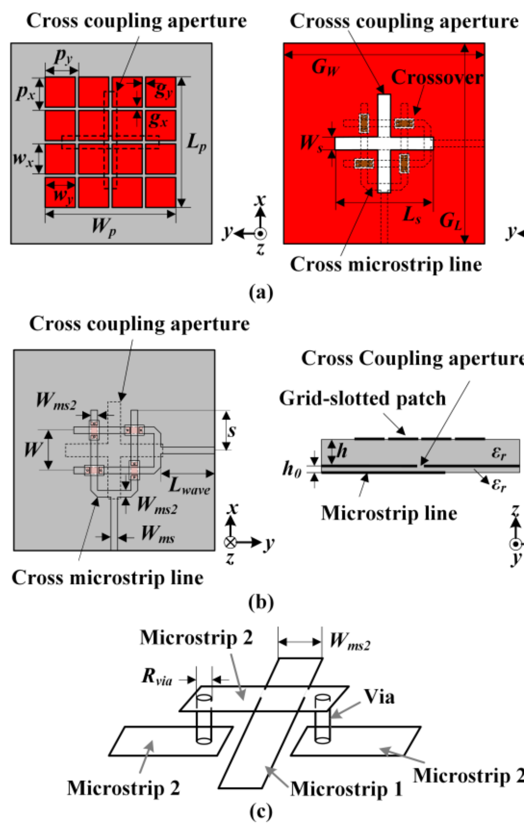

Fig. 2. Geometry of the proposed grid-slotted microstrip antenna: (a) top view of the radiating patch and GND, (b) bottom view of the feeding structure and side view of the overall structure, and (c) stereograph of the crossover.

Table 1: Optimized dimension of the proposed antenna (Unit: mm)

p_x	p_y	g_x	g_y	W_p	L_p	G_L	G_W	W_s
10	10	1	1	39	39	60	60	3.8
W	s	W_{ms}	W_{ms2}	L_{wave}	h	h_0	L_s	R_{via}
8	10	1.85	1.75	15.5	3.25	0.813	30	0.17

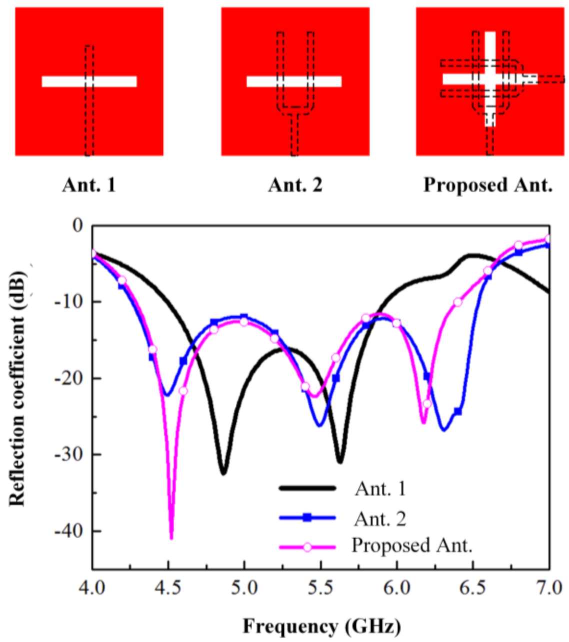

Fig. 3. Design evolution and simulated reflection coefficients.

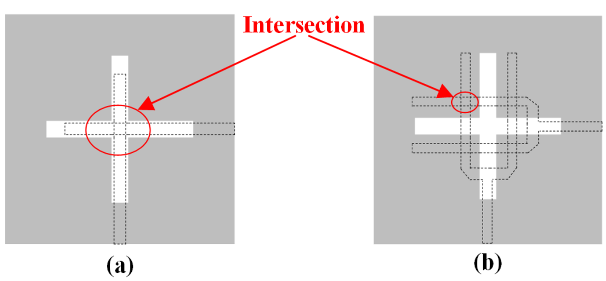

Fig. 4. Cross feeding structure: (a) with two orthogonal straight microstrip lines, and (b) with two orthogonal Y-shaped microstrip lines.

In the curve of Fig. 5 (a), three resonances appear at the frequencies of 4.5 GHz, 5.5 GHz, and 6.3 GHz. Snapshots of the vector electric field distributions at these three resonances are depicted in Figs. 5 (b)-(d). In Fig. 5 (b), it can be clearly seen that the E-field distribution is the TM_{10} mode of conventional patch antenna and meanwhile, there are very strong E-fields in the grid slots along y-axis between two adjacent small square units. There are two resonances for the higher order mode. The resonances at 5.5 GHz and 6.3 GHz have almost the same electric field distributions (Figs. 5 (c)-(d)), named as antiphase TM_{20} mode. The directions of the E-field of the coupled aperture are antiparallel. The mode sketches at different resonance frequencies are inserted in Fig. 5 (a).

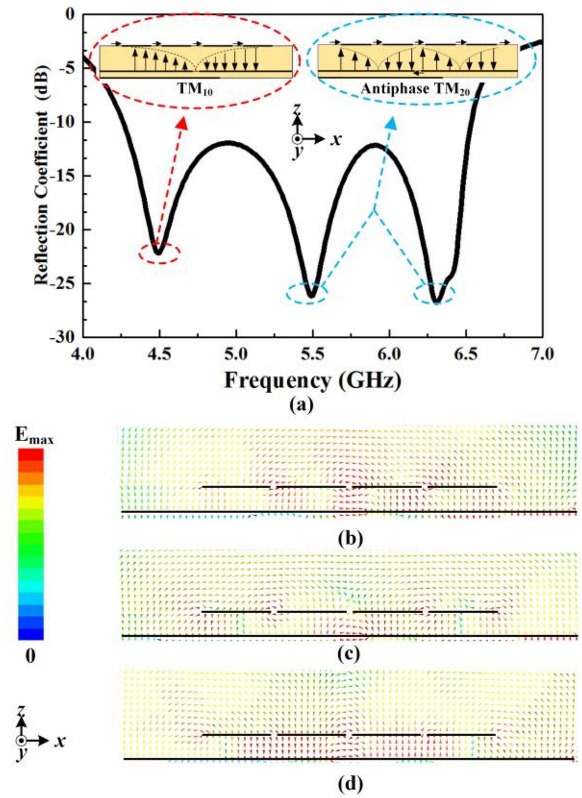

Fig. 5. Simulated reflection coefficient and E-field distribution of the proposed antenna. (a) Simulated reflection coefficient and sketches of the resonant modes. The vector electric field distributions at (b) 4.5 GHz, (c) 5.5 GHz, and (d) 6.3 GHz.

III. PROTOTYPE AND MEASUREMENTS

The numerical results illustrated in this study are obtained using the commercial software High Frequency Structure Simulator V15 (HFSS 15.0). Specifically, the frequency-domain solver with a Finite Element Method (FEM) algorithm is selected. During the simulation procedure, the solution frequency is 5.5 GHz and minimum converged passes is 2 with the converged precision of 0.02. For measurement, the Agilent E5071B vector network analyzer is used to measure the reflection and transmission coefficients. The ETS-LindgrenAMS8500 anechoic chamber is used to test the radiation performance.

A prototype of the proposed dual-polarized grid-slotted microstrip antenna (Proposed Ant.) is fabricated and measured, and Figs. 6 (a)-(c) show the photographs. The antenna prototype has the same dimensions with those listed in Table 1. The measured reflection and transmission coefficients at two ports are illustrated in Fig. 6 (d), also agreeing well with the simulated ones. The deviations may be mainly caused by manufacturing error, especially the thin air gap between upper and lower dielectrics. The achieved -10-dB impedance bandwidths are 4.23-6.62 GHz (44.1%) for port 1 and 4.26-6.61 GHz (43.2%) for port 2. The measured transmission coefficient between two ports is lower than -16 dB in the whole band.

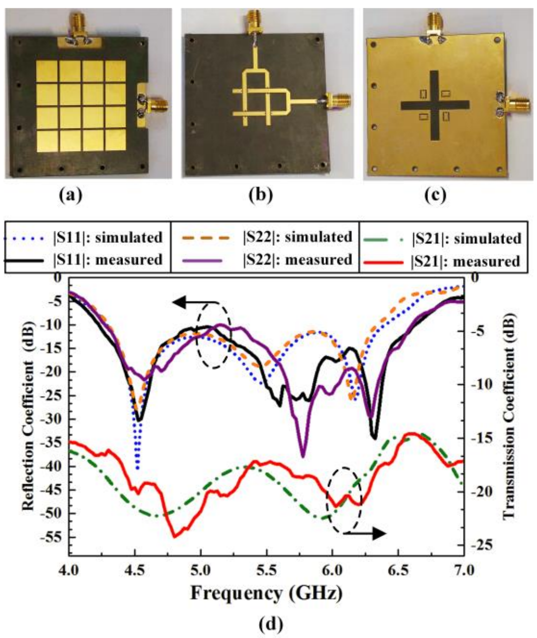

Fig. 6. Photographs and measured results of the fabricated Proposed Ant. (a) Top view, (b) bottom view, (c) the ground plane and cross coupling apertures in the GND layer, and (d) simulated and measured reflection and transmission coefficients.

Figures 7 and 8 show the simulated and measured normalized radiating patterns at 4.5 GHz, 5.5 GHz, and 6.3 GHz at two ports. The measured cross-polarization levels are less than -18 dB in the E-plane and -20 dB in the H-plane for port 1; -19 dB in the E-plane and –18 dB in the H-plane for port 2. Figure 9 (a) shows the simulated and measured gain and efficiency. For port 1, the simulated gain ranges from 6.9 to 10.4 dBi and the efficiency is higher than 89%, and the measured gain ranges from 6.4 to 10.1 dBi. For port 2, the simulated gain ranges from 6.9 to 10.5 dBi and the efficiency is higher than 80%, and the measured gain ranges from 6.5 to 10.3 dBi. The differences between the maximum gain and minimum gain are 3.7 dBi and 3.8 dBi, respectively. The gain variations are accepted (less than 4 dB) in the whole operating impedance bandwidth. The proposed antenna can be regarded as a binary array when operating at antiphase TM_{20} mode. Therefore, the gain at TM_{10} mode is lower than the gain at antiphase TM_{20} mode. In Fig. 9 (b), the envelope correlation coefficients (ECC) between the two ports is also presented, which can quantitatively evaluate the MIMO performance. The ECC of two ports can be calculated by the complex radiation far field and the formulation is given in equations (1) and (2) [13]. The ECC is less than 0.07 in the whole operating bandwidth. Comparing with the benchmark value of ECC less than 0.5 [14-15], the proposed dual-polarized antenna achieves an excellent MIMO performance:

$$\rho_e \approx |\rho_c|^2 = \left|\frac{\oiint A_{12}(\theta,\varphi)\sin\theta\, d\theta\, d\varphi}{\oiint A_{11}(\theta,\varphi)\sin\theta\, d\theta\, d\varphi \cdot \oiint A_{22}(\theta,\varphi)\sin\theta\, d\theta\, d\varphi}\right|^2, \quad (1)$$

where

$$A_{ij} = E_{\theta,i}(\theta,\varphi)\cdot E^*_{\theta,j}(\theta,\varphi) + E_{\varphi,i}(\theta,\varphi)\cdot E^*_{\varphi,j}(\theta,\varphi). \quad (2)$$

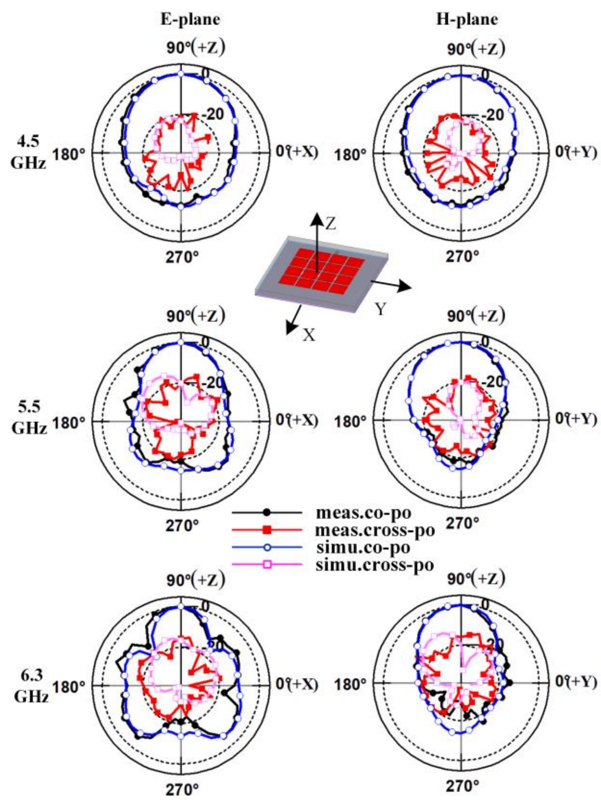

Fig. 7. Simulated and measured normalized radiating patterns at port 1 of the Proposed Ant. at 4.5 GHz, 5.5 GHz and 6.3 GHz.

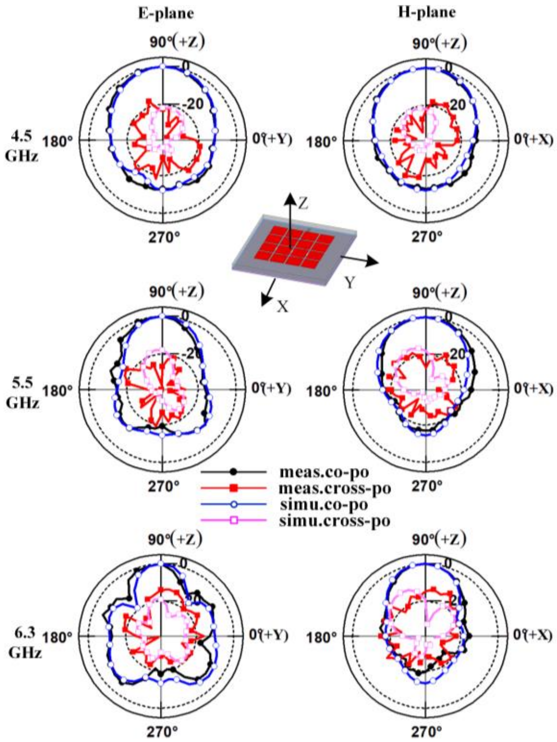

Fig. 8. Simulated and measured normalized radiating patterns at port 2 of the Proposed Ant. at 4.5 GHz, 5.5 GHz and 6.3 GHz.

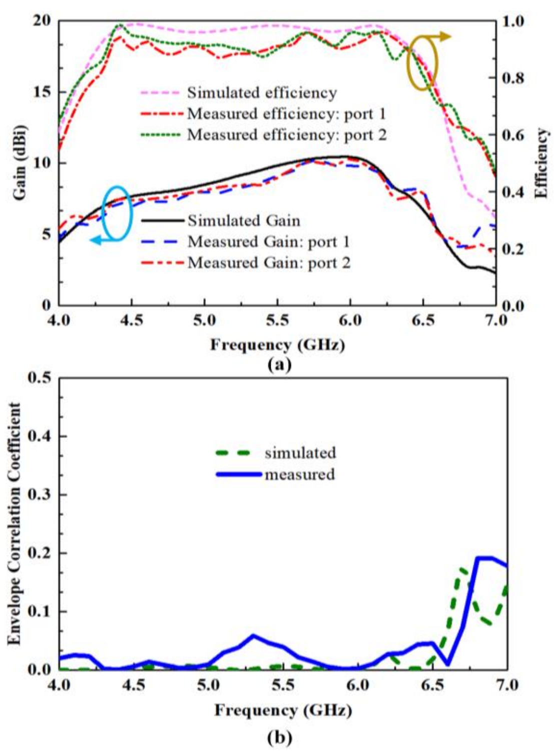

Fig. 9. Simulated and measured radiating performances of the Proposed Antenna. (a) Gain and efficiency, and (b) envelop correlation coefficients.

IV. CONCLUSION

In this paper, a dual-polarized grid-slotted microstrip antenna with enhanced bandwidth and low profile is proposed. The ingenious combination of the Y-shaped feeding structure and periodic radiating aperture is presented to enhance the bandwidth of the microstrip antenna significantly. The obtained results provide a guideline to design wideband microstrip antennas. Prototype of the proposed antenna is fabricated and measured. As shown in Table 2, compared with the existing broadband microstrip antennas [8,9,12], the proposed antenna can achieve wider bandwidth with low profile and meanwhile realize dual polarization. Compared with the existing dual-polarized antenna units [16-17] applied for base station, lower profile is observable. Up to 43% -10-dB bandwidth is obtained in our design, exhibiting possibilities to design dual-polarization low profile base station in wireless communication systems.

Table 2: Comparison of performances for various antennas (λ_0 is the centre operating wavelength in free space)

Antenna	Profile	BW	Polarization	Centre Frequency
Ref. [8]	0.07 λ_0	30.3%	Single	2.25 GHz
Ref. [9]	0.1 λ_0	36.8%	Single	30 GHz
Ref. [12]	0.06 λ_0	41%	Single	5.5 GHz
Ref. [16]	0.25 λ_0	54.5%	Dual	2.31 GHz
Ref. [17]	0.24 λ_0	45%	Dual	2.22 GHz
Proposed	**0.06 λ_0**	**43%**	**Dual**	**5.50 GHz**

ACKNOWLEDGMENT

This work was supported by the National Natural Science Foundation of China 61771280, and in part by Natural Science Foundation of Beijing Manipulate under Contract 4182029.

REFERENCES

[1] Q.-X. Chu, D. L. Wen, and Y. Luo, "A broadband ±45◦ dual-polarized antenna with Y-shaped feeding structure," *IEEE Trans. Antennas Propag.*, vol. 63, no. 2, pp. 483-490, Feb. 2015.

[2] Z. Bao, Z. Nie, and X. Zong, "A broadband dual-polarization antenna element for wireless commun-ication base station," *in Proc. IEEE Asia Pacific Conf. Antennas and Propagation*, pp. 144-146, 2012.

[3] K. M. Luk and H. Wong, "A new wideband unidirectional antenna element," *Int. J. Microw. Opt. Technol.*, vol. 1, no. 1, pp. 2098-2101, July 2006.

[4] O. Amjad, S. W. Munir, S. T. Imeci, and A. O. Ercan, "Design and implementation of dual band microstrip patch antenna for WLAN energy harvesting system," *Applied Computational Electro-magnetic Society (ACES) Journal*, vol. 33, no. 7,

pp. 746-751, July 2018.

[5] R. Garg, P. Bhartia, I. Bahl, and A. Ittipiboon, *Microstrip Antenna Design Handbook*. Boston, MA, USA: Artech House, 2001.

[6] E. Chang, S. A. Long, and W. F. Richards, "An experimental investigation of electrically thick rectangular microstrip antennas," *IEEE Trans. Antennas Propag.*, vol. 34, no. 6, pp. 767-772, June 1986.

[7] T. Huynh and K. F. Lee, "Single-layer single-patch wideband microstrip antenna," *Electron. Lett.*, vol. 31, no. 16, pp. 1310-1312, Aug. 1995.

[8] F. Yang, X. X. Zhang, X. Ye, and Y. Rahmat-Samii, "Wide-band E-shaped patch antennas for wireless communications," *IEEE Trans. Antennas Propag.*, vol. 49, no. 7, pp. 1094-1100, July 2001.

[9] S. Mestdagh, W. De Raedt, and G. A. E. Vandenbosch, "CPW-fed stacked microstrip antennas," *IEEE Trans. Antennas Propag.*, vol. 52, no. 1, pp. 74-83, Jan. 2004.

[10] N.-W. Liu, L. Zhu, W.-W. Choi, and X. Zhang, "A low-profile aperture-coupled microstrip antenna with enhanced bandwidth under dual resonance," *IEEE Trans. Antennas Propag.*, vol. 65, no. 3, pp. 1055-1062, Mar. 2017.

[11] A. U. Zaman, L. Manholm, and A. Derneryd, "Dual polarised microstrip patch antenna with high port isolation," *Electron. Lett.*, vol. 43, no. 10, pp. 551-552, Sep. 2007.

[12] W. Y. Sun, Y. Li, Z. Z. Zhang, and Z. H. Feng, "Broadband and low-profile microstrip antenna using strip-slot hybrid structure," *IEEE Antennas Wireless Propag. Lett.*, vol. 16, pp. 3118-3121, 2017.

[13] Z. Zhang, *Antenna Design for Mobile Devices*, 2nd Edition, Hoboken, NJ, USA: Wiley, 2017.

[14] J. M. Lee, K. B. Kim, H. K. Ryu, and J. M. Woo, "A compact ultrawideband MIMO antenna with WLAN band-rejected operation for mobile devices," *IEEE Antennas Wireless Propag. Lett.*, vol. 11, pp. 990-993, 2012.

[15] H. Minseok and C. Jaehoon, "Small-size printed strip MIMO antenna for next generation mobile handset application," *Microw. Opt. Technol. Lett.*, vol. 53, no. 2, pp. 48-352, 2011.

[16] D.-Z. Zheng and Q.-X. Chu, "A wideband dual-polarized antenna with two independently controllable resonant modes and its array for base-station applications," *IEEE Antennas Wireless Propag. Lett.*, vol. 16, pp. 2014-2017, 2017.

[17] Y. Y Jin and Z. W Du, "Broadband dual-polarized F-probe fed stacked patch antenna for base stations," *IEEE Antennas Wireless Propag. Lett.*, vol. 14, pp. 1121-1124, 2015.

Wangyu Sun received the B.S. degrees from Tsinghua University, in 2016. He is currently working toward the Master degree in Electrical Engineering at Tsinghua University. His current research interests include broadband antennas, low profile antennas and dual polarized antennas.

Yue Li received the B.S. degree in Telecommunication Engineering from the Zhejiang University, Zhejiang, China, in 2007, and the Ph.D. degree in Electronic Engineering from Tsinghua University, Beijing, China, in 2012. He is currently an Associate Professor in the Department of Electronic Engineering at Tsinghua University. In June 2012, he was a Postdoctoral Fellow in the Department of Electronic Engineering, Tsinghua University. In December 2013, he was a Research Scholar in the Department of Electrical and Systems Engineering, University of Pennsylvania. He was also a Visiting Scholar in Institute for Infocomm Research (I2R), A*STAR, Singapore, in 2010, and Hawaii Center of Advanced Communication (HCAC), University of Hawaii at Manoa, Honolulu, HI, USA, in 2012. Since January 2016, he has been with Tsinghua University, where he is an Assistant Professor. He has authored and coauthored over 90 journal papers and 45 international conference papers, and holds 15 granted Chinese patents. His current research interests include metamaterials, plasmonics, electromagnetics, nanocircuits, mobile and handset antennas, MIMO and diversity antennas, and millimeter-wave antennas and arrays. He was the recipient of the Issac Koga Gold Medal from URSI General Assembly in 2017; the Second Prize of Science and Technology Award of China Institute of Communications in 2017; the Young Scientist Awards from the conferences of ACES 2018, AT-RASC 2018, AP-RASC 2016, EMTS 2016, URSI GASS 2014; the Best Paper Awards from the conferences of CSQRWC 2018, NCMMW 2018 and 2017, APCAP 2017, NCANT 2017, ISAPE 2016, and ICMMT 2016; the Outstanding Doctoral Dissertation of Beijing Municipality in 2013, and the Principal Scholarship of Tsinghua University in 2011. He is serving as the Associate Editor of IEEE Transactions on Antennas and Propagation, IEEE Antennas and Wireless Propagation Letters and Computer Applications in Engineering Education, also as the Editorial Board of Scientific Report.